

## Effects of polarization on equilibrium and dynamic properties of ionic systems\*

G. Jacucci

*Centre Européen de Calcul Atomique et Moléculaire, Faculté des Sciences, 91 Orsay, France  
and Gruppo Nazionale de Struttura della Materia, Consiglio Nazionale della Ricerche, Istituto di Fisica, Università di Roma, Rome, Italy*

I. R. McDonald

*Department of Chemistry, Royal Holloway College, Egham, Surrey, England*

A. Rahman

*Argonne National Laboratory, Argonne, Illinois 60439*

(Received 26 March 1975)

Molecular-dynamics calculations are reported for systems of ions in which the contribution to the interionic forces arising from polarization is taken explicitly into account. Two models of polarization are considered: a modification of that used for alkali-halide molecules by Tosi and Doyama and a simplified version of the shell model of lattice dynamics. In each case the effects of polarization are superimposed on an underlying rigid-ion pair potential of the type proposed by Tosi and Fumi. Calculations of the phonon spectra show that use of either model leads to agreement with experimental data on solid NaCl, which is considerably better than that achieved with the Tosi-Fumi potential alone; good results are also obtained for solid KI. Calculations for molten KI based on the shell model show that the effect of polarization in the liquid state is to increase significantly the diffusion coefficients, particularly that of the positive ion, and decrease the shear viscosity, but the effect on electrical conductivity is almost negligible. These results are broadly consistent with the known adequacy of the rigid-ion-model to account for the transport coefficients of molten alkali halides. Polarization is also shown to lead to a reduction in the characteristic frequencies and a considerably increased damping of collective longitudinal-optic-type modes in the liquid. The effect on other collective modes is less pronounced.

### I. INTRODUCTION

It is well known that the dynamical properties of ionic solids cannot be fully understood in terms of rigid-ion models. In general, account must also be taken of the polarization of the ions by the internal electric field. For example, in crystals such as NaI, KBr, and NaCl, a particularly striking effect of polarization is to reduce significantly the frequencies of the optical modes of vibration. Polarization also plays an important part in determining the high-frequency dielectric behavior of such materials.

The effects of polarization in ionic crystals have been extensively studied by the established methods of lattice dynamics. At present, however, these methods can be usefully applied only when anharmonicity can be treated as a small perturbation. Therefore little is known about the importance of polarization at very high temperature. In the case of liquids, of course, the theoretical problem is even more severe.

An obvious way to study the properties of systems of polarizable ions, at least in the classical approximation, is through a computer "experiment." A number of papers have now appeared<sup>1-6</sup> in which computer simulation is used in the calculation of equilibrium and dynamic properties of molten ionic salts, but in these the problem of polarization has been almost entirely ignored.

The purpose of the present paper is to report the results of a series of molecular-dynamics calculations in which the contribution from polarization is included explicitly in the interionic forces. We have limited our calculations to the alkali halides, but the methods used may easily be applied to other salts.

The straightforward approach to the problem is to compute the total electric field acting on the ion and use the polarizability appropriate to a free ion (or a crystal polarizability) to calculate the resulting induced dipole moment. In this simple model the static and high-frequency dielectric constants are linked by the second Szigeti relation, but in practice, for the alkali-halide crystals, this relation is not at all closely obeyed.<sup>7,8</sup> Deviations from the Szigeti relation can be accounted for by introducing a short-range mechanical polarizability, so that the effective polarizability (electronic plus mechanical) becomes a function of the distance between ions, being less than its free-ion value at small separations. The damping of the polarizability should be coupled to the short-range interionic repulsion, because both effects originate in the overlap of the outer electron clouds. In order to describe the coupling, we must use a model which is not only realistic but also sufficiently simple to incorporate in molecular-dynamics calculations without an unacceptable increase in computing effort. Two models are

TABLE I. Parameters in the interionic potentials.  $b = 3.38 \times 10^{-13}$  erg;  $c_{++} = 1.25$ ,  $c_{+-} = 1.0$ , and  $c_{--} = 0.75$ .

Salt	$\sigma_+$ (Å)	$\sigma_-$ (Å)	$\lambda$ (Å)	$C_{++}$ ( $10^{-60}$ erg cm <sup>6</sup> )	$C_{--}$ ( $10^{-60}$ erg cm <sup>6</sup> )	$C_{+-}$ ( $10^{-60}$ erg cm <sup>6</sup> )	$D_{++}$ ( $10^{-76}$ erg cm <sup>8</sup> )	$D_{--}$ ( $10^{-76}$ erg cm <sup>8</sup> )	$D_{+-}$ ( $10^{-76}$ erg cm <sup>8</sup> )	$\alpha_+$ ( $10^{-24}$ cm <sup>-3</sup> )	$\alpha_-$ ( $10^{-24}$ cm <sup>-3</sup> )	$q_+/e$	$q_-/e$	$k_+$ ( $10^6$ erg cm <sup>-2</sup> )	$k_-$ ( $10^6$ erg cm <sup>-2</sup> )
NaCl	1.170	1.585	0.317	1.68	116	11.2	0.8	233	13.9	0.24	2.63	0	-3.17	...	0.690
KI	1.463	1.907	0.355	24.3	403	82	24	1130	156	...	...		-3.85	...	0.333

described in this paper. One of these was originally introduced by Tosi and Doyama<sup>7</sup> in work on alkali-halide molecules; the other is a simplified version of the shell model of lattice dynamics.<sup>8</sup> We shall show that in a certain approximation the two models are equivalent.

Specific calculations are reported for NaCl and KI in both liquid and solid states. In each case the polarization is superimposed on an underlying potential of the Huggins-Mayer form, with parameters proposed by Tosi and Fumi.<sup>9</sup> The Huggins-Mayer potential in the generalized form used by Tosi and Fumi may be written as

$$\varphi(r_{ij}) = Q_i Q_j / r_{ij} + \varphi_{\text{rep}}(r_{ij}) + \varphi_{\text{dis}}(r_{ij}), \quad (1)$$

where  $Q_i$  and  $Q_j$  are the charges on ions labelled  $i$  and  $j$ . The term  $\varphi_{\text{rep}}$  represents the short-range repulsive interactions,

$$\begin{aligned} \varphi_{\text{rep}}(r_{ij}) &= A_{ij} \exp(-r_{ij}/\lambda) \\ &= bc_{ij} \exp[(\sigma_i + \sigma_j)/\lambda] \exp(-r_{ij}/\lambda), \end{aligned} \quad (2)$$

and  $\varphi_{\text{dis}}$  is the contribution from Van der Waals dipole-dipole and dipole-quadrupole dispersion forces,

$$\varphi_{\text{dis}}(r_{ij}) = -C_{ij}/r_{ij}^6 - D_{ij}/r_{ij}^8. \quad (3)$$

Values used for the parameters in (2) and (3) are listed in Table I.

We wish to emphasize that our primary interest lies in the general question of assessing the importance of polarization in determining static and dynamic properties of a simple class of ionic materials and not in presenting results for specific systems. In any case, given the known inadequacies of the Tosi-Fumi potentials for the liquid state,<sup>1,3,6</sup> it seems unlikely that our results for molten KI have more than qualitative significance. For the crystals, on the other hand, the potentials are more reliable, having been fitted originally to solid-state data. Furthermore, the consequences of polarization in the crystals are dramatic and well understood, and plentiful experimental data are available to check the reliability of a model. For these reasons we attach particular importance to our calculations on the low-temperature solids.

The outline of the paper is as follows: In Sec.

II we review the models we have used and discuss the relation between them. In Sec. III we present the results we have obtained for the crystals at room temperature and, in the case of NaCl, at a temperature close to the melting point. The calculations we have made for liquid KI are discussed in Sec. IV, and some concluding remarks and suggestions for future work are given in Sec. V.

## II. MODELS OF POLARIZABLE IONS

### A. Model of Tosi and Doyama

As we have already remarked, the model of Tosi and Doyama<sup>7</sup> was originally introduced to describe the properties of alkali-halide molecules. Initially, therefore, it is convenient to discuss the method from the same point of view. Quadrupoles and higher-order multipoles are ignored, and the induced dipoles as functions of the ionic separation are given by

$$\begin{aligned} \mu_+(r) &= \alpha_+ [e/r^2 + 2\mu_-(r)/r^3], \\ \mu_-(r) &= \alpha_- [e/r^2 + 2\mu_+(r)/r^3 - B(r)], \end{aligned} \quad (4)$$

where  $\alpha_+$  and  $\alpha_-$  are the electronic polarizabilities. The total potential energy is therefore

$$\varphi_{\text{TD}}(r) = \varphi(r) - \frac{1}{2} [\mu_+(r) + \mu_-(r)] e/r^2 + \frac{1}{2} \mu_-(r) B(r), \quad (5)$$

where  $\varphi(r)$  is the Tosi-Fumi potential.

The function  $B(r)$  plays the role of a mechanical polarizability which opposes the electrically induced dipole moment and controls the growth of polarization over a range of interionic separations close to the equilibrium distance. For the sake of simplicity the short-range polarizability is assumed to act only on the negative ion, which in the alkali halides generally has a much larger electronic polarizability. The damping of the polarization is assumed to be proportional to the short-range repulsive part of the potential; we therefore set  $B(r) = \xi \varphi_{\text{rep}}(r)$ , where the positive constant  $\xi$  is determined by the deviation of the Szegeti effective charge from unity through an expression given by Tosi and Doyama.

It is straightforward to generalize the model to the many-body case for use in molecular-dynam-

ics calculations. For speed in computing we have chosen to neglect the contribution from interactions between induced dipoles, and the damping function is assumed to operate only on the interaction between positive and negative ions. The neglect of dipole-dipole interactions means that iterations are not required, and the programming of the calculations is similar to that in the rigid-ion case. In practice, however, the method does not work, except at very low temperatures. In general a "catastrophe" occurs, manifesting itself in a very rapid rise in temperature of many orders of magnitude. To understand why this happens, it is instructive to return to the problem of two ions. Eliminating  $\mu_+$  and  $\mu_-$  from Eq. (5) by means of (4), we find (the ion-dipole approximation) that

$$\begin{aligned} \varphi_{TD}(r) = & \varphi(r) - \frac{1}{2}(e^2/r^4)(\alpha_+ + \alpha_-) + (e/r^2)\alpha - \xi\varphi_{rep} \\ & - \frac{1}{2}\alpha_- \xi^2 [\varphi_{rep}(r)]^2. \end{aligned} \quad (6)$$

For NaCl the function  $\varphi_{TD}(r)$  passes through a maximum at  $r = 1.78 \text{ \AA}$  and then decreases rapidly. It is important to realize that this occurs as a result of the growth of the *final* term on the right-hand side of (6), the term in  $r^{-4}$  becoming dominant only at very small values of  $r$  ( $\sim 0.1 \text{ \AA}$ !). Thus replacement of the exponential repulsive term in the Tosi-Fumi potential by an inverse power term would not eliminate the "catastrophe." The source of the difficulty is the fact that the hoped-for balance between mechanical and electronic polarizabilities is maintained only over a rather small range of  $r$ ; as  $r$  decreases, the mechanical effect overwhelms the electrical one. The situation is illustrated in Fig. 1; inclusion of the dipole-dipole terms leads to no significant improvement.

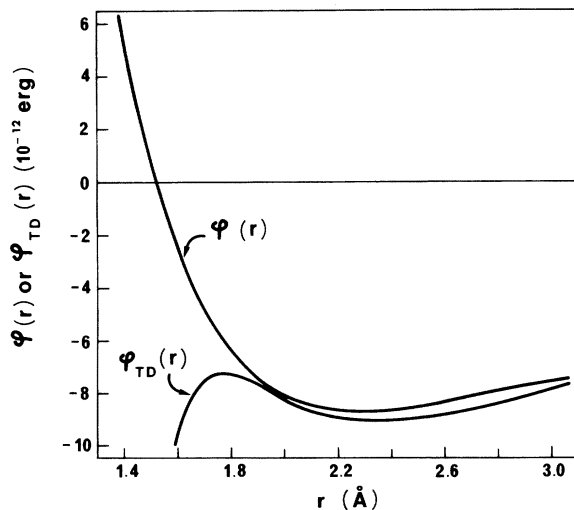


FIG. 1. Tosi-Fumi potential for NaCl and Tosi-Doyama pair potential, Eq. (6).

To make progress we have adapted the Tosi-Doyama model in an *ad hoc* manner by introducing a short-range repulsion which has the effect of precisely cancelling the "catastrophic" term in the two-body potential, the growth of polarization at short range now being controlled by the *third* term on the right-hand side of (6). With this trick if was found possible to carry out molecular-dynamics calculations at high temperatures. The modification we use was suggested to us by the work of Brumer and Karplus<sup>10</sup> on diatomic alkali halides. Brumer and Karplus show that a consistent perturbation treatment which includes terms of second order in the potential and second order in the overlap leads to a pair potential which is similar in form to Eq. (6), except that the "catastrophic" term, being of fourth order in the overlap, does not appear. Thus in the case of an isolated ion pair our model (apart from the minor question of dipole-quadrupole dispersion terms) becomes identical to that of Brumer and Karplus. While this comparison does not constitute a justification for our approach, we believe it lends it an added credibility. A similar proposal has been made by Schofield,<sup>11</sup> but in a different context.

#### B. Shell model

In the simple shell model<sup>8</sup> of lattice dynamics the total charge of a polarizable ion is assumed to be divided between a core and a massless spherical shell, the latter being bound to the core through a harmonic potential. In addition, the short-range repulsive forces are assumed to act through the shells. Let  $\vec{r}_i$  be the coordinates of the core of ion  $i$ , and let  $\vec{s}_i$  be the coordinates of the center of the shell relative to its own core. Then if  $q_i$  is the charge on the shell ( $Q_i - q_i$  being the charge on the core) and  $k_i$  is the spring constant in the harmonic potential, the total potential energy of a system of polarizable ions may be written

$$\begin{aligned} \Phi = & \sum_{i < j} \left[ \frac{(Q_i - q_i)(Q_j - q_j)}{r_{ij}} + \frac{(Q_i - q_i)q_j}{|\vec{r}_{ij} - \vec{s}_j|} + \frac{q_i(Q_j - q_j)}{|\vec{r}_{ij} + \vec{s}_i|} \right. \\ & \left. + \frac{q_i q_j}{|\vec{r}_{ij} + \vec{s}_{ij}|} + A_{ij} \exp\left(-\frac{|\vec{r}_{ij} + \vec{s}_{ij}|}{\lambda}\right) \right. \\ & \left. + \varphi_{dis}(r_{ij}) \right] + \frac{1}{2} \sum_i k_i s_i^2, \end{aligned} \quad (7)$$

where  $\vec{r}_{ij} = \vec{r}_i - \vec{r}_j$  and  $\vec{s}_{ij} = \vec{s}_i - \vec{s}_j$ . In this model the polarization of the ions corresponds to a bodily shift of the shell (representing the electron cloud) relative to the core (representing the nucleus). No effort has been made to incorporate refinements which allow for deformation of the shell.<sup>12</sup> It

would be more consistent to assume that the dispersion forces also act through the shell, but in practice the point is not important.

The task of solving the full dynamical problem of the shell model is a formidable one. We therefore proceed by expanding  $\Phi$  in powers of the shell displacements.<sup>13</sup> Subsequent differentiation with respect to  $\vec{r}_i$  yields the force on the  $i$ th particle, and the equations of motion of the core can be integrated numerically in the usual way. The shells, being of zero mass, are assumed to adjust themselves instantaneously in such a way as to satisfy the condition  $\vec{\nabla}_s \Phi = 0$ .

Truncation of the expansion at first order involves a degree of inconsistency because it is necessary to retain the final term in (7), representing the induction energy of the dipoles, even though it is quadratic in the shell displacements. The first-order result corresponds to neglecting all additional electrostatic contributions except the ion-dipole terms, whereas the full shell model contains all higher-order multipole interactions. In this approximation the equilibrium displacement of the  $i$ th shell is given by

$$k_i \vec{s}_i = \sum_{j \neq i} \vec{r}_{ij} \left[ \frac{Q_j q_i}{r_{ij}^3} + \frac{A_{ij}}{\lambda r_{ij}} \exp\left(\frac{-r_{ij}}{\lambda}\right) \right]. \quad (8)$$

Thus the shell displacements are functions only of the positions of the cores. However, the meth-

$$k_i \vec{s}_i = \sum_{j \neq i} \left\{ \frac{1}{r_{ij}^3} [Q_j q_i (\vec{r}_{ij} + \vec{s}_i) - q_i q_j \vec{s}_j] - \frac{3\vec{r}_{ij}}{r_{ij}^5} [Q_j q_i (\vec{r}_{ij} \cdot \vec{s}_i) - q_i q_j (\vec{r}_{ij} \cdot \vec{s}_j)] + \frac{A_{ij}}{\lambda r_{ij}} \exp\left(\frac{-r_{ij}}{\lambda}\right) [\vec{r}_{ij} + \vec{s}_{ij} - \vec{r}_{ij} (\vec{r}_{ij} \cdot \vec{s}_{ij})] \left( \frac{1}{r_{ij}^2} + \frac{1}{\lambda r_{ij}} \right) \right\}. \quad (10)$$

Thus each  $\vec{s}_i$  is dependent on all  $\vec{s}_j$  and iterative methods must be used. Fortunately, the first-order result (8) already provides a good initial guess, and when this is used as input in the calculation of the shell coordinates one iteration is sufficient.

There is now no "catastrophe," even at very high temperatures. To understand the improvement relative to the first-order calculation we consider once more the problem of two ions in isolation. For simplicity we treat the case of a pair of oppositely charged ions in which the positive ion is taken as nonpolarizable ( $q_+ = 0$ ). This approximation is a reasonable one for most of the alkali halides and is used throughout the shell-model calculations we report below. The equilibrium displacement of the shell of the negative ion now turns out to be

$$s_-(r) = \left( \frac{eq_-}{r^2} - \frac{d\varphi_{\text{rep}}(r)}{dr} \right) / \left( k_- + \frac{2eq_-}{r^3} + \frac{d^2\varphi_{\text{rep}}(r)}{dr^2} \right), \quad (11)$$

od again breaks down at high temperatures, the source of the "catastrophe" being the same as in the Tosi-Doyama model. The potential for an isolated pair is now

$$\begin{aligned} \varphi_{\text{SM}}^{(1)}(r) = & \varphi(r) - \frac{1}{2} \frac{e^2}{r^4} \left( \frac{q_1^2}{k_1} + \frac{q_2^2}{k_2} \right) \\ & - \frac{1}{r^2} \left( \frac{Q_2 q_1}{k_1} + \frac{Q_1 q_2}{k_2} \right) \frac{d\varphi_{\text{rep}}(r)}{dr} \\ & - \frac{1}{2} \left( \frac{1}{k_1} + \frac{1}{k_2} \right) \left( \frac{d\varphi_{\text{rep}}(r)}{dr} \right)^2. \end{aligned} \quad (9)$$

This has substantially the same form as Eq. (6). We see, in particular, the appearance of a "catastrophic" term, i.e., the final term on the right-hand side. Comparison of the two equations enables us to identify the electronic polarizabilities as  $\alpha_i = q_i^2/k_i$ ; a complete equivalence cannot be established only because the mechanical polarizability of the positive ion is ignored in the Tosi-Doyama model.

We could again avoid the difficulty by including an additional term in the interionic potential, but we can achieve a similar result in a less arbitrary way by carrying the expansion of  $\Phi$  to second order in  $\vec{s}_i$ . The equilibrium value of the shell displacement is in that case given by

allowing us to define an  $r$ -dependent polarizability as

$$\alpha(r) = \frac{q_- s_-(r)}{e/r^2}. \quad (12)$$

Equation (11) shows that the model possesses the properties we require. At large  $r$  we recover the free-ion polarizability, i.e.,  $\alpha(r) \rightarrow q_-^2/k_-$ , and at small  $r$  the dipole moment vanishes linearly with  $r$ , i.e.,  $q_- s_-(r) \rightarrow \frac{1}{2} q_- r$ . Finally, at intermediate value of  $r$ , the presence of the term  $d^2\varphi_{\text{rep}}/dr^2$  in the denominator ensures that the induced dipole moment remains small. In first order, by contrast, the denominator consists only of the term  $k_-$ . The effective polarizability of the  $\text{Cl}^-$  ion in the  $\text{NaCl}$  molecule, as given by Eq. (12), is plotted in Fig. 2, and is seen to decrease rapidly for  $r \lesssim 3 \text{ \AA}$ , later reversing sign and then passing smoothly to zero.

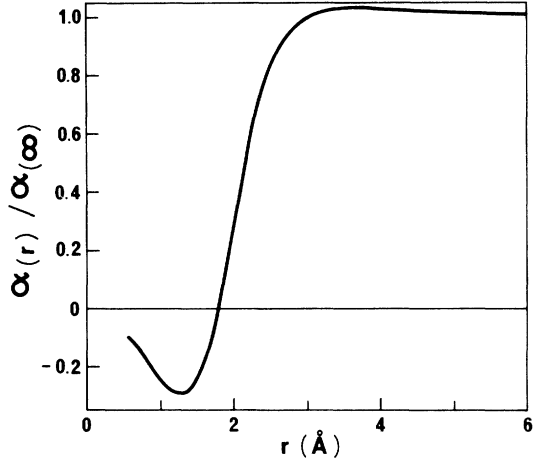


FIG. 2. Effective polarizability of  $\text{Cl}^-$  in the NaCl molecule according to the second-order shell model, Eq. (12).

### III. APPLICATION TO SOLIDS

We have used both the modified Tosi-Doyama (MTD) model and the second-order shell (SM2) model in simulations of NaCl at temperatures of approximately 300 and 1150 K; the latter temperature is greater than the melting point of the real crystal (1073 K). The choice of NaCl was influenced by the fact that the dynamics of the Tosi-Fumi rigid-ion (RI) model, and in particular the phonon dispersion curves, had already been studied in great detail by molecular dynamics.<sup>14</sup> We have also made calculations of KI at room temperature for both the RI and SM2 models. The MTD and SM2 parameters which were used are listed in Table I. Note that we have ignored the polarization of the positive ion in the calculations with the shell model. The parameters for the negative ions are taken from the work of Sangster,<sup>15</sup> except that we have used a somewhat smaller value for the spring constant of KI. On the other

hand, we choose not to adopt the force constants proposed by Sangster, but prefer to retain the potential of Tosi and Fumi. The reason is simply that our immediate goal is not to achieve an exact fit to the experimental phonon frequencies but to develop a model which will account for a wider range of phenomena. We are therefore reluctant, at this stage, to abandon the Tosi-Fumi potential, as we know that it describes satisfactorily most of the thermodynamic properties of the alkali-halide crystals.

In Table II we give some technical details of the calculations:  $N$  is the number of ions in the molecular-dynamics cell,  $\Delta t$  is the time step in the numerical integrations, and  $N_t$  is the total number of steps in the run. For the sake of completeness we include some results obtained previously for the RI model of NaCl. To maintain satisfactory conservation of energy (to better than one part in  $10^3$ ) we have used a smaller value of  $\Delta t$  in the calculations for the polarizable models than in the RI case.

Some relevant equilibrium properties are also tabulated in Table II:  $U$ , the total internal energy;  $U_p$ , the contribution to  $U$  which arises from polarization terms; and  $\langle r_i^2 \rangle^{1/2}$ , the rms displacements of the ions. The polarization energy is very small at room temperature and rises by a factor of about 4.5 between 300 and 1150 K. The rms displacements in the polarizable systems are close to the values predicted by Buyers and Smith<sup>16</sup> on the basis of a deformation dipole model. They are also consistently larger than the values obtained in the RI calculations. Results obtained with the two polarizable models agree satisfactorily with each other.

The major effort in the calculations on solids has been directed at the computation of the dynamical structure factor  $S(\vec{k}, \omega)$ . We have made this calculation in the manner of Levesque *et al.*,<sup>17</sup> that is, we have computed  $S(\vec{k}, \omega)$  directly from the classical expression

TABLE II. Molecular-dynamics calculations on solid alkali halides.

Salt	Model	$N$	$\Delta t$ ( $10^{-14}$ sec)	$N_t$ ( $10^3$ )	$T$ (K)	$V$ ( $\text{cm}^3 \text{ mol}^{-1}$ )	$-U$ ( $\text{kJ mol}^{-1}$ )	$\frac{100U_p}{U}$	$\frac{100\langle r_+^2 \rangle^{1/2}}{d}$	$\frac{100\langle r_-^2 \rangle^{1/2}}{d}$
NaCl	RI <sup>a</sup>	216	0.70	6	301.7	27.60	769.4	...	8.2	8.0
	RI <sup>a</sup>	216	0.70	28.8	1153.0	31.37	742.0	...	20.6	19.5
	MTD	64	0.38	4.3	301.6	27.60	769.0	0.16	12.6	12.1
	MTD	64	0.20	8	1158.3	31.37	745.5	0.75	27.1	21.5
	SM2	216	0.35	1	306.3	27.60	769.5	0.16	12.6	11.0
	SM2	216	0.20	4	1153.5	31.37	740.2	0.74	24.3	23.6
KI	RI	216	1.80	2	300.8	53.12	630.4	...	9.5	8.2
	SM2	216	0.80	2	330.2	53.12	627.5	0.51	13.1	10.8

<sup>a</sup> Reference 14. Note that  $d$  is the nearest-neighbor distance in the lattice.

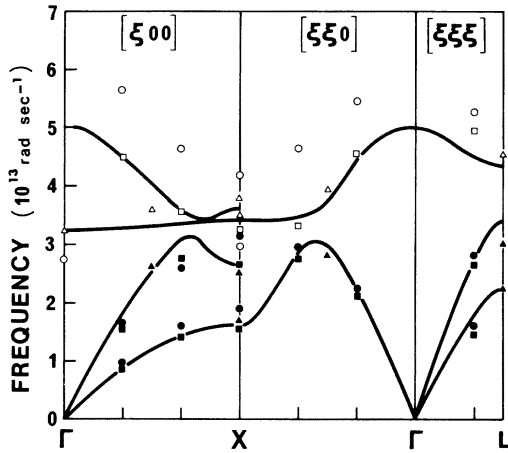


FIG. 3. Phonon dispersion curves in NaCl. The curves are experimental data from Ref. 18 and the points are molecular-dynamics results:  $\circ$ , RI optic;  $\bullet$ , RI acoustic;  $\triangle$ , MTD optic;  $\blacktriangle$ , MTD acoustic;  $\square$ , SM2 optic;  $\blacksquare$ , SM2 acoustic.

$$S(\vec{k}, \omega) = \lim_{\tau \rightarrow \infty} \frac{1}{N\tau} \int_0^\tau e^{i\omega t} \rho_{\vec{k}}(t) dt \int_0^\tau e^{-i\omega t'} \rho_{-\vec{k}}(t') dt' \\ = \frac{1}{N} \lim_{\tau \rightarrow \infty} \frac{1}{\tau} |\rho_{\vec{k}}(\omega)|^2, \quad (13)$$

rather than indirectly as a Fourier transform of the density-density correlation function. The density operator appearing in Eq. (13) may be written as

$$\rho_{\vec{k}}(t) = \rho_{\vec{k}}^+(t) + \rho_{\vec{k}}^-(t), \quad (14)$$

where

$$\rho_{\vec{k}}^+(t) = \sum_{i \in +} e^{i\vec{k} \cdot \vec{r}_i(t)}, \quad \rho_{\vec{k}}^-(t) = \sum_{j \in -} e^{i\vec{k} \cdot \vec{r}_j(t)}. \quad (15)$$

Thus the calculation of  $S(\vec{k}, \omega)$  reduces to that of the calculation of partial dynamical structure factors and we can write, in an obvious notation,

$$S(\vec{k}, \omega) = S_{++}(\vec{k}, \omega) + S_{--}(\vec{k}, \omega) + 2S_{+-}(\vec{k}, \omega). \quad (16)$$

The cross section for the inelastic scattering of neutrons may be obtained by weighting the partial quantities by appropriate products of the nuclear scattering lengths, and the phonon frequencies can then be identified with the peaks in the spectrum recorded at constant  $\vec{k}$ .

In Fig. 3 we show the low-temperature experimental dispersion curves for NaCl and the results obtained by molecular dynamics for the RI, MTD, and SM2 models. For the sake of clarity we have omitted the transverse branches in the [110] direction and the TO mode in the [111] direction. As anticipated, the inclusion of polarization leads to

a large decrease in the frequencies of the LO modes and a marked improvement in agreement with experimental results.<sup>18</sup> (The latter were obtained at 80 K.) Little change is seen in the frequencies of the acoustic modes. Some discrepancies remain, particularly at the X-point, in the case of SM2, and at the point  $(\frac{1}{2}, 0, 0)$  in the case of MTD. At the point  $(\frac{1}{3}, \frac{1}{3}, \frac{1}{3})$  there is only a small reduction in the LO frequency in the SM2 calculations, but this is a region which is always difficult to fit with a shell model. The MTD model gives better results than SM2 for the frequencies of the TO mode in the [100] direction, which necessarily means, because the TO modes exhibit only weak dispersion, that it also gives a better fit to the LO branch in the [100] direction near the X-point. Some caution is necessary, however, in comparing the MTD and SM2 calculations because the very small number of ions used in studying the MTD model may influence the results. Overall, however, the calculations show that the two models which we have used reproduce satisfactorily the known effects of polarization in solids, though further improvements are required if quantitatively accurate results are required.

Between room temperature and a temperature close to the melting point the phonons show very considerable broadening, but it remains possible to identify a peak frequency. The shifts in frequency are all negative and as large as 30%; the smallest shifts, approximately 10%, are in the LO modes. Similar behavior is seen in all three models. Detailed comparison with experiment is not possible because of the lack of neutron-scattering data at high temperatures. The TO ( $\vec{k} = 0$ ) phonon shows a shift of approximately 25% (RI) and 30% (MTD and SM2), which is rather large in comparison with the experimental value<sup>19</sup> of 11%, based on infrared measurements, over the temperature range 300–750 K. It is likely, however, that the effects of anharmonicity would lead to a rather rapid change in frequency with temperature as the melting point is approached. We find, for example, that in the RI model the frequency shift at 950 K is only 16% relative to the room-temperature value.<sup>14</sup>

We have also measured the frequencies of selected phonons in KI at approximately 300 K for comparison with the experimental values<sup>20</sup> at 90 K. The results are listed in Table III and are broadly in line with those obtained for NaCl. The TO frequencies are poorly predicted, but this fault is already apparent in the RI results. Polarization considerably improves the fit to the LO and TA frequencies in the [100] direction, but overall the results are somewhat inferior to those obtained for NaCl.

TABLE III. Frequencies of selected phonons in KI as calculated with the models RI and SM2, and from experiment.

Point	Mode	Frequency ( $10^{12}$ rad sec $^{-1}$ )		
		RI	SM2	Expt.
$(\frac{1}{3}, 0, 0)$	LO	30.0	23.0	24.0
	TO	17.5	16.5	20.0
	LA	7.9	7.8	8.2
	TA	3.7	3.3	3.1
$(\frac{2}{3}, 0, 0)$	LO	25.0	21.0	21.0
	TO	18.5	16.5	21.0
	LA	13.0	12.5	12.0
	TA	6.3	5.0	5.3
$(1, 0, 0)$	LO	24.0	18.0	21.0
	TO	18.0	17.0	21.0
	LA	13.0	9.5	10.0
	TA	7.4	5.0	5.6
$(\frac{1}{3}, \frac{1}{3}, 0)$	LO	29.0	25.5	24.5
	LA	9.5	9.5	10.0
$(\frac{2}{3}, \frac{2}{3}, 0)$	LO	21.5	19.5	21.0
	LA	12.0	11.0	11.5
$(\frac{1}{3}, \frac{1}{3}, \frac{1}{3})$	LO	28.5	29.0	25.0
	TO	16.0	15.5	19.0
	LA	12.0	12.0	11.0
	TA	7.2	6.8	8.5

The calculations we report in this section show that the models we propose simulate with reasonable accuracy the known effects of polarization in the solid state. We may therefore use the same models with some confidence in studying the properties of liquids, for which much less is known about the importance of polarization.

#### IV. APPLICATION TO MOLTEN KI

In order to assess the role played by polarization in determining the properties of molten salts, we have made two lengthy molecular-dynamics calculations on liquid KI, one with the RI potential and one with the SM2 model. The choice both of system and of model is necessarily somewhat arbitrary. We chose KI in preference to NaCl because the polarizability of  $I^-$  is greater than that of  $Cl^-$ , though it does not follow that the effects

of polarization are greater in KI, because the relative sizes of the ions must also be taken into account. Larger effects may be expected in NaI, but the choice of such a system presents the problem that the necessary reduction in  $\Delta t$  relative to that used in the RI calculations is correspondingly greater, making the computations considerably more expensive. As we wish to calculate transport coefficients, long runs appear to be inevitable. In the interests of obtaining maximum information we have sacrificed some numerical accuracy by working with a time step in the polarizable case which is only one-half that used in the RI calculations. In consequence we have experienced some difficulty in maintaining a stable temperature, though the total energy does remain constant, with fluctuations of the order of one part in 500. To eliminate any tendency to a long-term drift in temperature we have adjusted the velocities of the ions appropriately, never by more than a few parts in a thousand and by usually much less, at intervals of approximately 80 steps, this interval being determined by the length of the "segments" discussed below. (A subsequent period is always allowed for equilibration.) Such small adjustments are unlikely to lead to any serious error. As a check, we carried out an independent run with a time step reduced by a factor of 4 in which no drift in temperature was seen and found essentially identical results for thermodynamic properties and radial distribution functions. No similar difficulty was encountered in the solid-state calculations, where the time step used for the RI computations (again, twice that for SM2) is superfluously small.

Some details of the calculations are given in Table IV. For comparison we note that the triple point<sup>21</sup> of KI occurs at  $T=958$  K,  $V=67.9$  cm $^3$  mol $^{-1}$ . The results reported show that polarization contributes only 2.2% of the potential energy of the system. Nonetheless, there is a significant effect on the structure. In Figs. 4-6 we make a comparison between the RI and SM2 results for the three core-core radial distribution functions,  $g_{++}(r)$ ,  $g_{--}(r)$ , and  $g_{+-}(r)$ . We see that in the polarizable melt the peaks in  $g_{++}(r)$  and  $g_{--}(r)$  are flatter than in the RI case. In  $g_{+-}(r)$  the main peak is shifted inwards by

TABLE IV. Molecular-dynamics calculations on molten KI;  $N=216$ ,  $V=68.97$  cm $^3$  mol $^{-1}$ . Values in parentheses are experimental results.

Model	$\Delta t$ ( $10^{-14}$ sec)	$N_t$ ( $10^3$ )	$T$ (K)	$-U$ (kJ mol $^{-1}$ )	$\frac{100U_p}{U}$	$\sigma$ (mho cm $^{-1}$ )	$D_+$ ( $10^{-5}$ cm $^2$ sec $^{-1}$ )	$D_-$	$\eta$ (cP)
RI	1.8	8.5	989.0	585.0	...	1.42	4.5	3.7	1.06
SM2	0.9	6.7	958.0	584.6	2.2	1.38 (1.38)	7.5	4.3	0.88 (1.40)

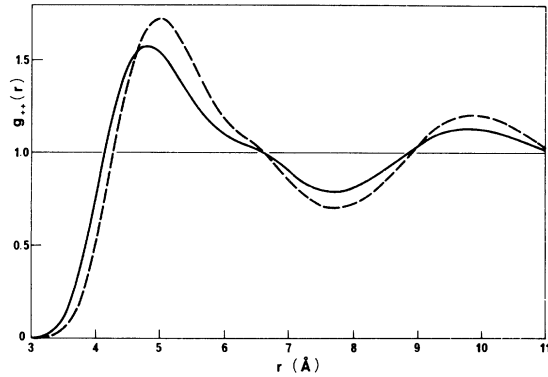


FIG. 4. Radial distribution function  $g_{++}(r)$  in molten KI. Dashed curve: RI; full curve: SM2.

approximately  $0.3 \text{ \AA}$ , but the later oscillations are almost perfectly in phase with those in the RI function. In  $g_{--}(r)$  the first peak is shifted slightly outwards, although the distance of closest approach is smaller; at larger values of  $r$  there is little change. There is a "kink" in  $g_{++}(r)$  between the two first peaks and a similar but less pronounced feature in  $g_{--}(r)$ . However, in the shell-shell distribution function  $g_{ss}(r)$  the kink is barely perceptible. The function  $g_{++}(r)$  is virtually unaltered by polarization, except that the peaks at large  $r$  are slightly flattened. The core-shell distribution function  $g_{s+}(r)$  has a main peak which is shifted inwards by approximately  $0.1 \text{ \AA}$ , but the distance of closest approach is not altered.

We now turn to a discussion of the results we have obtained on the dynamical properties of the RI and polarizable models. For both systems we have measured a number of transport coefficients: the diffusion constants for positive and negative ions  $D_+$  and  $D_-$ , the electrical conductivity  $\sigma$ , and the shear viscosity  $\eta$ . We have also obtained some information on the form of the longitudinal and

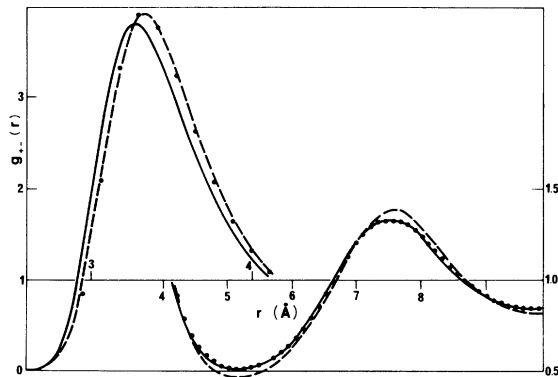


FIG. 5. Radial distribution function  $g_{+-}(r)$  in molten KI. Dashed curve: RI; points: SM2; full curve:  $g_{s+}(r)$ .

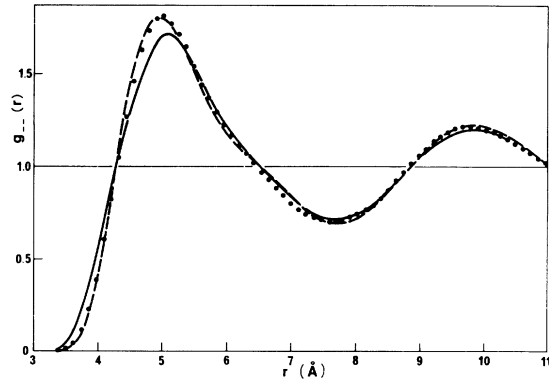


FIG. 6. Radial distribution function  $g_{--}(r)$  in molten KI. Dashed curve: RI; full curve: SM2; points:  $g_{ss}(r)$ .

transverse current-current correlation functions of acoustic and optic character. By analogy with the phonon calculations we denote these functions, which in the liquid are dependent only on the magnitude of the vector  $\vec{k}$ , by the symbols  $C_{LA}(k, t)$ ,  $C_{LO}(k, t)$ ,  $C_{TA}(k, t)$ , and  $C_{TO}(k, t)$ . The diffusion coefficients were obtained by integrating the velocity autocorrelation functions, calculated in the standard way. The current-current correlation functions were determined directly from small perturbations of the trajectories of the ions by methods which are described in detail elsewhere.<sup>22</sup>

In summary, we apply to each ion at  $t=0$  a small ( $\sim 1 \text{ V cm}^{-1}$ ) force which acts in the  $x$  direction, say, with a magnitude which varies sinusoidally along either the  $x$  direction, for longitudinal modes, or along the  $z$  direction, for transverse modes. In modes of acoustic character the force acts on all ions in the same sense, and for optic modes it acts in opposite sense on ions of opposite charge. The force acts only at  $t=0$  and thereafter the calculation proceeds as normal. The current induced is then compared with that occurring when the system begins from the same initial conditions but the force is not applied. This procedure is repeated for a number of such pairs of segments and a simple argument based on linear-response theory shows that the *mean* difference in current after a time  $t$  is proportional to the appropriate time-correlation function. The transport coefficients  $\sigma$  and  $\eta$  represent two special cases, being determined by the integrals, respectively, of  $C_{TO}(k, t)$  and  $C_{TA}(k, t)$  in the limit  $k=0$ . The function  $C_{TO}(0, t)$  can be computed directly; here the appropriate force is one which is independent of position but acts in opposite senses, along the same axis, on positive and negative ions. The transverse acoustic mode  $C_{TA}(k, t)$  can be studied only at finite  $k$  and the value of  $\eta$  obtained by extrapolation. The length of each segment is taken to be the same and



equal to 80 steps, and no information can be gained on time correlations having a longer lifetime. Note that the number of time steps given in Table IV refers to the number of independent configurations, so that the number actually generated was twice as large, once with the perturbations applied and once without.

Our results on the transport coefficients are summarized in Table IV, together with the available experimental values.<sup>21</sup> We estimate the statistical errors in the calculations to be approximately 3% for the diffusion coefficients and 5% for  $\sigma$  and  $\eta$ . To place these data in perspective, it is necessary to recall briefly the conclusions reached by Ciccotti *et al.*,<sup>23</sup> who have made molecular-dynamics calculations of the transport coefficients of six alkali-halide liquids on the basis of the RI model. Although there are some anomalies, and the experimental data are incomplete, the results may be summarized as follows: For the electrical conductivity the agreement is generally very good to the extent that in most cases the discrepancies are within the limits of statistical error. The calculated viscosities are everywhere too high, except in the case of KI for which the experimental value is much higher than for any other salt. In general, however, the data on viscosity are consistent with the fact that with one exception ( $I^-$  in NaI) the computed diffusion coefficients are too high. Furthermore, the discrepancies are considerably larger for  $D_+$  than for  $D_-$ .

With these points in mind the data presented in Table IV are seen to have a number of satisfactory features. First, the electrical conductivity is scarcely altered by the inclusion of polarization, so that the good agreement with experiment is retained. This is not the result of a fortuitous cancellation of errors, by which we mean that the corresponding autocorrelation function is almost unaltered. What is fortuitous is the fact that we now find agreement to three significant figures with the experimental result. In the case of the viscosity the effect of polarization is to reduce its value by 17%. Of course, in the case of KI this actually *increases* the discrepancy with experiment, but KI, as we already remarked, is an anomalous case. Furthermore, our results are consistent with the fact that  $D_+$  and  $D_-$  both show a marked increase when polarization is included, the increase being larger for  $D_+$  than for  $D_-$ . Unfortunately there are no experimental diffusion coefficients available for KI, but our calculations are in broad agreement with data on alkali halides taken as a group.

The increase in both  $D_+$  and  $D_-$  is associated with rather striking changes in the corresponding

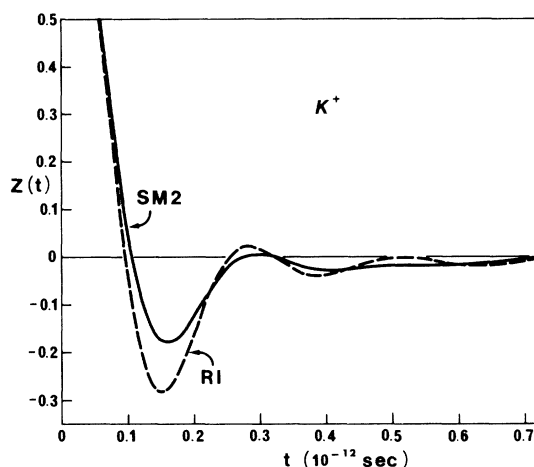


FIG. 7. Normalized velocity autocorrelation function of  $K^+$  in molten KI.

velocity autocorrelation functions. The normalized correlation functions  $Z(t)$  are plotted in Figs. 7 and 8. We see that polarization results in a heavy damping of the strongly oscillatory behavior which is characteristic of the RI functions. This is particularly evident in the case of  $K^+$ , where the region of negative autocorrelation becomes considerably weaker when the negative ions are allowed to polarize; the effect on  $I^-$  itself is less pronounced. Negative autocorrelation of velocity corresponds to a backscattering motion which in molten salts arises both from geometric and electrostatic factors. The weakening of the backscattering effect in the polarizable model may reflect the fact that local charge neutrality can to some extent be maintained by displacement of

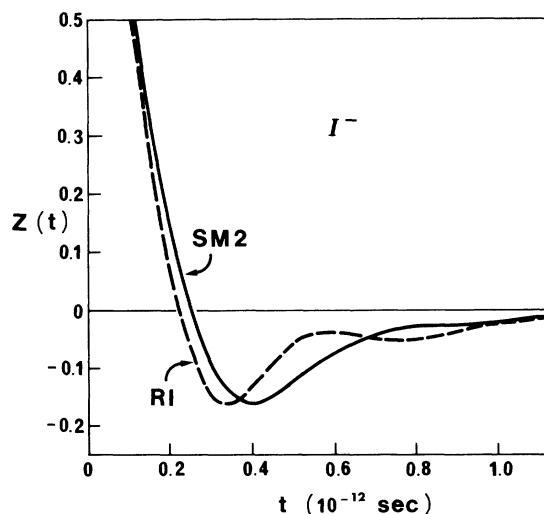


FIG. 8. Normalized velocity autocorrelation function of  $I^-$  in molten KI.

TABLE V. Characteristic frequencies of collective modes in molten KI.

Mode	Model	Frequency ( $10^{12}$ rad sec $^{-1}$ )			
		$n=0$	$n=1$	$n=2$	$n=3$
LO	RI		27.6	24.7	
	SM2		24.6	21.1	
TO	RI	13.8		13.8	
	SM2	14.7		13.0	
LA	RI		5.0	10.5	10.9
	SM2		4.8	9.2	9.7
TA	RI		<sup>a</sup>		5.9
	SM2		<sup>a</sup>		5.3

<sup>a</sup> No peak at nonzero frequency.

the electron cloud even when the ion is breaking through the cage of surrounding neighbors. In other words, the importance of the electrostatic factor may be reduced even though the geometric constraint remains.

The effect of polarization on the collective modes of the liquid is largely what is to be expected on the basis of the solid-state calculations. We have studied the various modes for several values of the wave number  $k = nk_{\min}$ , where  $k_{\min} = 0.27 \text{ \AA}^{-1}$  is the smallest accessible wave number in our periodic system. In Table V we list the characteristic frequencies associated with the various modes, which we identify with the peaks in the transforms of the appropriate correlation functions. The longitudinal-optic-type modes show clearly the negative shift in frequency which is typical of the LO modes in the solid. The

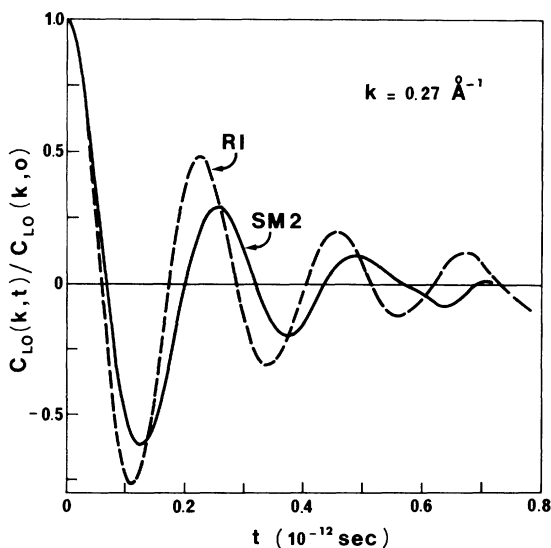


FIG. 9. Charge-charge correlation function in molten KI for the case  $n=1$ .

characteristic optic frequencies in solid and liquid are apparently very similar, which we can see by comparing the results for  $n=1$  and  $n=2$  with the phonon frequencies of Table IV at the points  $(\frac{1}{3}, 0, 0)$  and  $(\frac{2}{3}, 0, 0)$ . In fact, the change is rather greater than these figures suggest, because the phonon frequencies should be compared with the peak positions in the function  $\tilde{C}_{LO}(k, \omega)/\omega^2$  rather than in  $\tilde{C}_{LO}(k, \omega)$ ; this has the effect of displacing the liquid-state values towards lower frequency by about 5%. There is a much larger difference between solid and liquid in the case of the longitudinal-acoustic-type modes, where again we see a negative frequency shift arising from polarization.

Polarization also leads to an increased damping of the longitudinal-optic-type modes. In Figs. 9 and 10 we plot the function  $C_{LO}(k, t)$  for the cases  $n=1$  and  $n=2$ . The increase in relative damping with increasing  $k$  suggests that the fluctuations in charge density will cease to propagate at smaller values of  $k$  when the ions are polarizable, but we have no direct evidence on this point.

The effect of polarization on the transverse-optic-type modes is small, to which is related the fact that the change in  $\sigma$  is negligible. The shape of the function  $C_{TO}(k, t)$  also varies only slowly with increasing  $k$ . However, for  $n=1$  the transverse-acoustic-type correlation function  $C_{TA}(k, t)$  decays considerably more slowly in the polarizable system, an effect which is associated with the smaller value obtained for  $\eta$ . Shear waves are present in both models for  $n=3$ , with characteristic frequencies differing by approximately 10%. The damping of the shear waves is greater in the

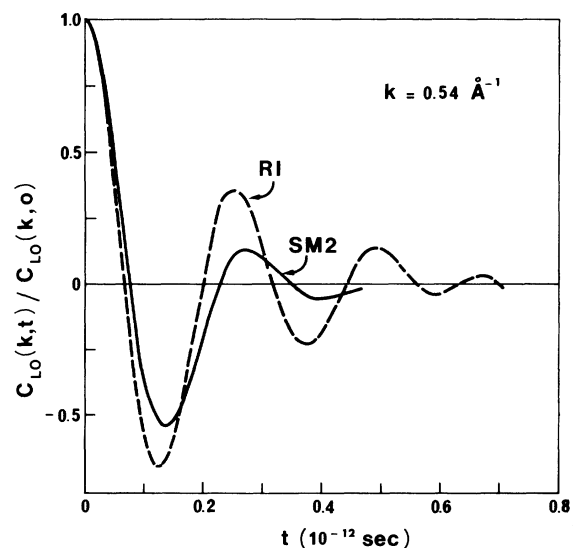


FIG. 10. Charge-charge correlation function in molten KI for the case  $n=2$ .

RI case, which again is a consequence of the difference in the viscosities of the two systems.

### V. CONCLUSIONS

We have devised two simple models which can be used in molecular-dynamics calculations of the properties of systems of polarizable ions. One is a modification of the diatomic model of Tosi and Doyama; the other is a version of the well-known shell model. In order to test the adequacy of the models we have used them in molecular-dynamics calculations of phonon frequencies in NaCl and KI crystals at room temperature, and find much-improved agreement with experimental data, particularly on the LO branches where the effects of polarization are known to be large. We have then used the shell-model program to calculate certain of the properties of molten KI for comparison with results obtained with a rigid-ion model. Some small but not insignificant structural effects are found. However, our main effort has been directed at the study of transport properties. We find a small decrease in shear viscosity for the polarizable system and a large increase in the diffusion coefficients, particularly in that of the positive ion. The electrical conductivity is essentially unaltered. The longitudinal collective modes of optic character are found to be more strongly damped when polarization is added and the characteristic frequencies are shifted to lower values. There is also some decrease in the frequencies associated with the longitudinal-acoustic modes. In the case of shear waves, however, the damping is greater in the rigid-ion model, an effect which is associated

with higher value of the viscosity.

Our results provide some detailed information of the way in which the properties of molten salts are modified by polarization of the ions, but many problems remain for future study. In particular, some improvement is needed in the models we have used so that better agreement is obtained for solid-state properties. Consideration should also be given to other systems, particularly LiI and NaI, for which the effects of polarization may be dramatic. A comprehensive study of the collective modes would also be of interest as it would supplement a number of recent calculations based on rigid-ion models.<sup>24</sup> Finally, some effort is needed to improve the algorithm used for the liquid-state calculations. We believe, however, that our work has established the main qualitative features of the role of polarization in simple ionic systems.

### ACKNOWLEDGMENTS

The work we have described was largely carried out during the course of a workshop on "Molecular dynamics of ionic systems," held at CECAM, Orsay. Our thanks go to Carl Moser, the director of CECAM, for making it possible for us to participate in this very successful meeting. It is also a pleasure to have this opportunity to thank our colleagues at the workshop, and Konrad Singer in particular, for their interest in the work. We also thank Giovanni Ciccotti for his invaluable help in carrying out the calculations on transport properties and M. L. Klein for a number of useful discussions and for pointing out the relevance of the work of Brumer and Karplus.

\*Work supported, in part, by the United Kingdom Science Research Council and the United States Atomic Energy Commission.

<sup>1</sup>L. V. Woodcock and K. Singer, *Trans. Faraday Soc.* **67**, 12 (1971).

<sup>2</sup>A. Rahman, R. H. Fowler, and A. H. Narten, *J. Chem. Phys.* **57**, 3010 (1972).

<sup>3</sup>D. J. Adams and I. R. McDonald, *J. Phys. C* **7**, 2761 (1974).

<sup>4</sup>F. Lantelme, P. Turq, B. Quentrec, and J. W. E. Lewis, *Mol. Phys.* **28**, 1537 (1974).

<sup>5</sup>J. P. Hansen and I. R. McDonald, *J. Phys. C* **7**, L384 (1974).

<sup>6</sup>J. W. E. Lewis and K. Singer, *JCS Faraday Trans. II* **71**, 41 (1975); J. W. E. Lewis, K. Singer, and L. V. Woodcock, *JCS Faraday Trans. II* **71**, 308 (1975).

<sup>7</sup>M. P. Tosi and M. Doyama, *Phys. Rev.* **160**, 716 (1967).

<sup>8</sup>B. J. Dick and A. W. Overhauser, *Phys. Rev.* **112**, 90 (1958).

<sup>9</sup>M. P. Tosi and F. G. Fumi, *J. Phys. Chem. Solids* **25**, 45 (1964).

<sup>10</sup>P. Brumer and M. Karplus, *J. Chem. Phys.* **58**, 3903 (1973).

<sup>11</sup>P. Schofield, in Report of CECAM workshop on "Molecular dynamics of ionic systems," 1974 (unpublished).

<sup>12</sup>U. Schröder, *Solid State Commun.* **4**, 347 (1966).

<sup>13</sup>G. Jacucci, I. R. McDonald, and K. Singer, *Phys. Lett.* **50A**, 141 (1974).

<sup>14</sup>G. Jacucci, M. L. Klein, and I. R. McDonald, *J. Phys. C* **36**, L97 (1975).

<sup>15</sup>M. J. L. Sangster, *J. Phys. Chem. Solids* **34**, 355 (1973).

<sup>16</sup>W. J. L. Buyers and T. Smith, *J. Phys. Chem. Solids* **29**, 1051 (1968).

<sup>17</sup>D. Levesque, L. Verlet, and J. Kürkijarvi, *Phys. Rev. A* **7**, 1690 (1973).

<sup>18</sup>G. Raunio, L. Almqvist, and R. Stedman, *Phys. Rev.* **178**, 1496 (1969).

<sup>19</sup>J. E. Mooij, W. G. van de Bunt, and J. E. Schrijvers, *Phys. Lett.* **28A**, 573 (1969).

<sup>20</sup>G. Dolling, R. A. Cowley, C. Schittenhelm, and I. M.

Thorson, Phys. Rev. 147, 577 (1966).

<sup>21</sup>R. E. Young and J. P. O'Connell, Ind. Eng. Chem. Fund. 10, 418 (1971).

<sup>22</sup>G. Ciccotti and G. Jacucci, Phys. Rev. Lett. 35, 789 (1975).

<sup>23</sup>G. Ciccotti, G. Jacucci, and I. R. McDonald, Phys.

Rev. A 13, 426 (1976).

<sup>24</sup>J. P. Hansen and I. R. McDonald, Phys. Rev. A 11, 2111 (1975); unpublished calculation by J. R. D. Copley and A. Rahman (for RbBr) and E. M. Gosling and K. Singer (for NaCl).